

Semiconductor to Metal Transition, Dynamical Stability and Superconductivity of Strained Phosphorene

G. Q. Huang^{1,2}, Z. W. Xing^{2,3}

¹*Department of Physics, Nanjing Normal University, Nanjing 210023, China*

²*National Laboratory of Solid State Microstructures,
Nanjing University, Nanjing 210093, China*

³*Department of Materials Science and Engineering,
Nanjing University, Nanjing 210093, China*

Abstract

Very recently, field-effect transistors based on few-layer phosphorene crystals with thickness down to a few nanometres have been successfully fabricated, triggering interest in this new functional two-dimensional material. In this work, we apply the first-principles calculations to studying the evolution of electronic structures and lattice dynamics with vertical strain for monolayer and bilayer phosphorenes. It is found that, by changing the thickness of phosphorene or the strain applied on it, its band gap width can be well tuned, and there will appear a transition from semiconductor to metal. In particular, the bilayer phosphorene may become a good BCS superconductor by adjusting the interlayer distance, in which the interlayer van der Waals coupling is favorable to the dynamical stability against strain.

PACS numbers: 63.22.Np, 73.61.Cw, 74.78.-w

I. INTRODUCTION

Black phosphorus (BP) is the most stable allotrope of the element phosphorus and has many interesting physical properties. BP can server as the electrode material for Lithium-Ion batteries.^{1,2} Several structural phase transitions were found under pressure accompanied by semiconductor-semimetal-metal transition.^{3,4} Furthermore, it was reported that the BP single crystal shows superconductivity with T_C higher than 10K under high pressure.^{5,6} The structure of BP consists of puckered double layers, which are held together by weak van der Waals (vdW) force. This peculiar layer structure permits to employ mechanical exfoliation to extract thin black phosphorus from a bulk crystal. Recently, the few-layer black phosphorus (phosphorene) had been successfully exfoliated and used them to create field-effect transistors, which exhibit large current on-off ratios and high mobilities.⁷⁻⁹ The successful fabrication of this novel two-dimensional (2D) semiconducting material was soon paid amounts of attention and predicted to have a great potential for practical applications.^{10,11}

Bulk BP is a direct-gap semiconductor with a 0.33 eV band gap.¹² However, the band gap of phosphorene is predicted to be highly sensitive to its thickness and strain. Previous first-principles calculations show that the band gap ranges from 1.5 eV for a monolayer to 0.6 eV for a 5-layer.¹³ A 3% in-plane strain can change phosphorene from a direct-gap to an indirect-gap semiconductor,⁸ while a vertical compression can induce the semiconductor to metal transition.¹⁴ Strain is an effective method to tailor electronic properties for 2D semiconductors. For monolayer phosphorene (MLP) and bilayer phosphorene (BLP), whether there are different strain effects on electronic properties is one of the motivation of this study. Furthermore, due to the interlayer coupling bonded by weak van der Waals force, it is also interesting to see how bilayer phosphorene responses to the change of interlayer distance.

While there have been substantial works on the electronic properties of phosphorene, investigations on the vibrational properties of phosphorene are scarce. The Raman spectra was measured for the BP flake with thicknesses ranging from 1.6 nm to 9 nm.¹⁵ The phonon dispersion of MLP was calculated by first-principles calculations.^{10,16} The lattice vibrational modes of MLP with in-plane strain were also reported by Fei *et al.* through first-principles simulations.¹⁶ However, phosphorene has an anisotropic structure, whether it has different dynamical behavior for phosphorene with out-of-plane strain? This problem is our concern. We will pay particular attention to the dynamical stability of strained phosphorene in order

to better use them for practical application.

In this work, geometric structure, electronic structure and lattice dynamics of MLP and BLP under vertical strain are studied and compared by first-principles calculations. The calculated results show that the evolution behavior of band structure for MLP and BLP under vertical strain is different. The dynamical stable range of the strained BLP is wider than that of the strained MLP. Furthermore, we also find that BLP may become a good BCS superconductor by adjusting the interlayer distance.

II. COMPUTATIONAL DETAILS

The first-principles calculations have been performed within the density functional theory through the PWSCF program of the Quantum-ESPRESSO distribution.¹⁷ The ultrasoft pseudo-potential and general gradient approximation (GGA-PBE) for the exchange and correlation energy functional are used with a cutoff of 30 Ry for the expansion of the electronic wave function in plane waves. MLP and BLP are modeled using the slabs, which are separated by vacuum layer with the thickness of about 35 Å. For the electronic structure calculations, the Brillouin zone integrations are performed with a (8,10,1) wavevector k -space grid by using the first-order Hermite-Gaussian smearing technique. Within the framework of the linear response theory, the dynamical matrixes are calculated for special \mathbf{q} points in the two dimensional irreducible Brillouin zone and are Fourier interpolated throughout the full Brillouin zone. The dense (24,30,1) grid are used in the Brillouin zone integrations in order to produce the accurate electron-phonon (EP) interaction matrices. As BP presents a laminar crystal structure, vdW correction proposed by Grimme (DFT-D2) is included in our calculations.¹⁸

III. RESULTS AND DISCUSSION

A. Geometric structure under vertical strain

BP has a layered orthorhombic structure. Each sheet consists of an atomic double layers known as a puckered layer. The stacking of the puckered layer for BP is $ABAB \dots$ sequence with weak van der Waals bonding between layers. The edge of the puckered hexagon of A layer is located in the center of the puckered hexagon of B layer and vice versa. The

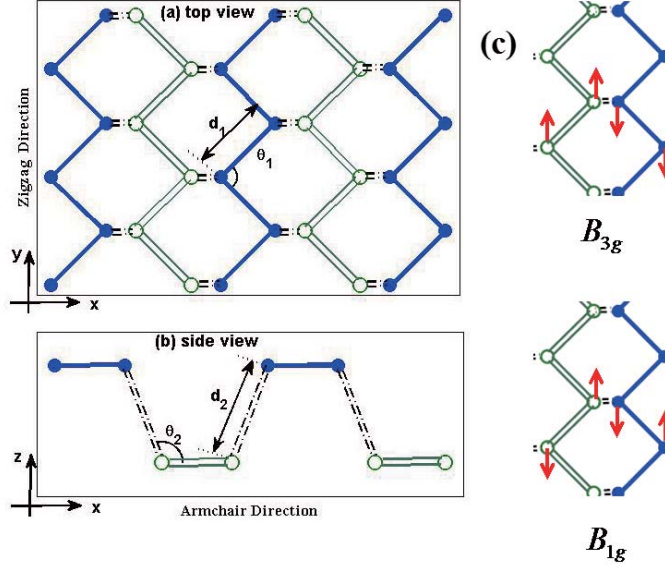


FIG. 1: The top (a) and side views (b) of the atomic structure of phosphorene. (c) Vibrational pattern of B_{3g} and B_{1g} modes.

top and side views of the atomic structure of a puckered layer are presented in Figs. 1 (a) and (b), respectively. Each layer may be viewed as consisting of armchair and zigzag chains along x and y , respectively. Each phosphorus atom is covalently bonded to three neighbors within the puckered layer. Our optimized bond lengths, bond angles (as labeled in Fig. 1) and lattice constants for BP are listed in Table 1. For comparison, the results without vdW correction for bulk BP are also listed in Table 1. It can be clearly seen that the inclusion of vdW interaction changes a and b parameters slightly, but reduces the c parameter substantially (about 0.6\AA). The overall best agreement with experimental¹⁹ and previous computational results²⁰ is achieved with inclusion of vdW correction.

For the free MLP and BLP (see Table 2), lattice constant b and bond lengths are very close to those in the bulk BP, while a and bond angles θ_2 are larger than those for the bulk BP. This fact shows that the increase of lattice constants a is not due to the change of bond lengths, but is due to the flattening of puckered layer. Next we concentrate mainly on

the strained phosphorene. The vertical strain is modeled by constraint z for the outmost layer atoms, the unit cell and other atomic positions are then relaxed. The strain is defined as $\sigma = \frac{h-h_0}{h_0}$, where h and h_0 are the thickness of the strained and the free phosphorene, respectively. The positive (negative) of σ corresponds to the tensile (compressive) strain. The obtained geometric parameters for MLP and BLP under vertical strain are listed in Table 2.

For the MLP, when tensile (compressive) strain is applied in the z direction, the lattice constant a decreases (increases) substantially. While the lattice constant b and the bond length d_1 show only a weak variation under strain, reflecting the rigidity of the strong covalent bonding along the zigzag direction. So the anisotropic geometric structure along armchair (x) and zigzag (y) directions result in their different responses to the vertical strain. With the decrease of thickness (h) of phosphorene, the bond length d_2 decreases and the bond angle θ_2 increases, reflecting the flattening of the puckered layer. It is need to mention that the range of strain studied here is not too large, the puckered character of structure still remains. The previous calculations by Rodin *et al.*¹⁴ showed that the monolayer approaches a plane square lattice configuration under severe compression.

For the BLP, when tensile strain is applied, the distance between puckered layers increases, while the covalent bonds within the puckered layer change slightly. And we also find that the geometric parameters of BLP are tend to those in the MLP when tensile strain is increased to 40%. This result is reasonable, since the coupling between puckered layers may be ignored at so large interlayer distance (about 6 Å). With increase of compressive strain applied, the change of geometric parameters of BLP is qualitatively same as in the case of MLP but with smaller magnitude. Unlike to that for the MLP, the lattice constant a of the BLP always increases whatever compressive or tensile strain is applied along z direction. This peculiar property is same to that observed in the bulk BP.²¹ This result implies that BLP has the same unusual mechanical response as bulk BP.

B. Electronic structures under vertical strain

The calculated band structures of the strained MLP and BLP are shown in Fig. 2. For the free MLP (Fig. 2c), the band dispersion along the major high symmetry directions compares very well with the previous calculations by Rodin *et al.*¹⁴ It is a direct band gap

semiconductor with the band gap energy about 0.83 eV. The top of the valence band and the bottom of the conduction band have predominantly p_z character mixed with p_x and s character. The band structure of the free BLP (Fig. 2h) has similar shape to that of MLP but with smaller gap energy (0.40 eV). The photoluminescence measurements¹⁵ and previous calculations¹³ indicated a thickness dependent band structure of the phosphorene.

The vertical strain effect on the electronic structure of MLP can be seen from (a) to (e) of Fig. 2. Both the compressive and tensile strains applied for the MLP can result in the transition from semiconductor to semimetal or metal. The band gap E_g located at Γ point keeps direct and decreases with the tensile strain, turning into zero when the tensile strain reaches 8% (Fig. 2d), and then converting into semimetal or metal (Fig. 2e) with increasing the tensile strain continuously. When compressive strain is applied, the band gap firstly keeps direct and increases slightly, but turns into indirect when the compressive strain reaches about 4%. Then indirect band gap decreases and turns into zero at about 25% compressive strain (Fig. 2b), and finally converting into semimetal or metal when the compressive strain continues to increase (Fig. 2a).

For the BLP, when tensile strain is applied, the band gap E_g keeps direct and increases until tends to the value in the free MLP. The corresponding band structure (Fig. 2i) is also similar to that of the free MLP (see Fig. 2c). Under small compressive strain (1%), the band gap soon turns into indirect and decreases with increasing the compressive strain. It turns into zero when the compressive strain reaches about 8% (Fig. 2g), and finally converts into metal (Fig. 2f).

The evolution of the band gap E_g with the strain for the MLP and BLP is summarized in Fig. 2j. The change of band gap is very extensive. So we can find that the electronic structure of thin BP is very sensitive to its thickness and the strain applied. This properties help to tailor materials in electronics. In order to better understand this novel 2D materials and use them for potential applications, next we turn to discuss the dynamical stability of the strained phosphorene.

C. Lattice vibration under vertical strain

The symmetry of phosphorene is described by the D_{2h} point group. For the MLP, the primitive cell contains four atoms, leading to 12 vibrational modes, i.e. nine optical and

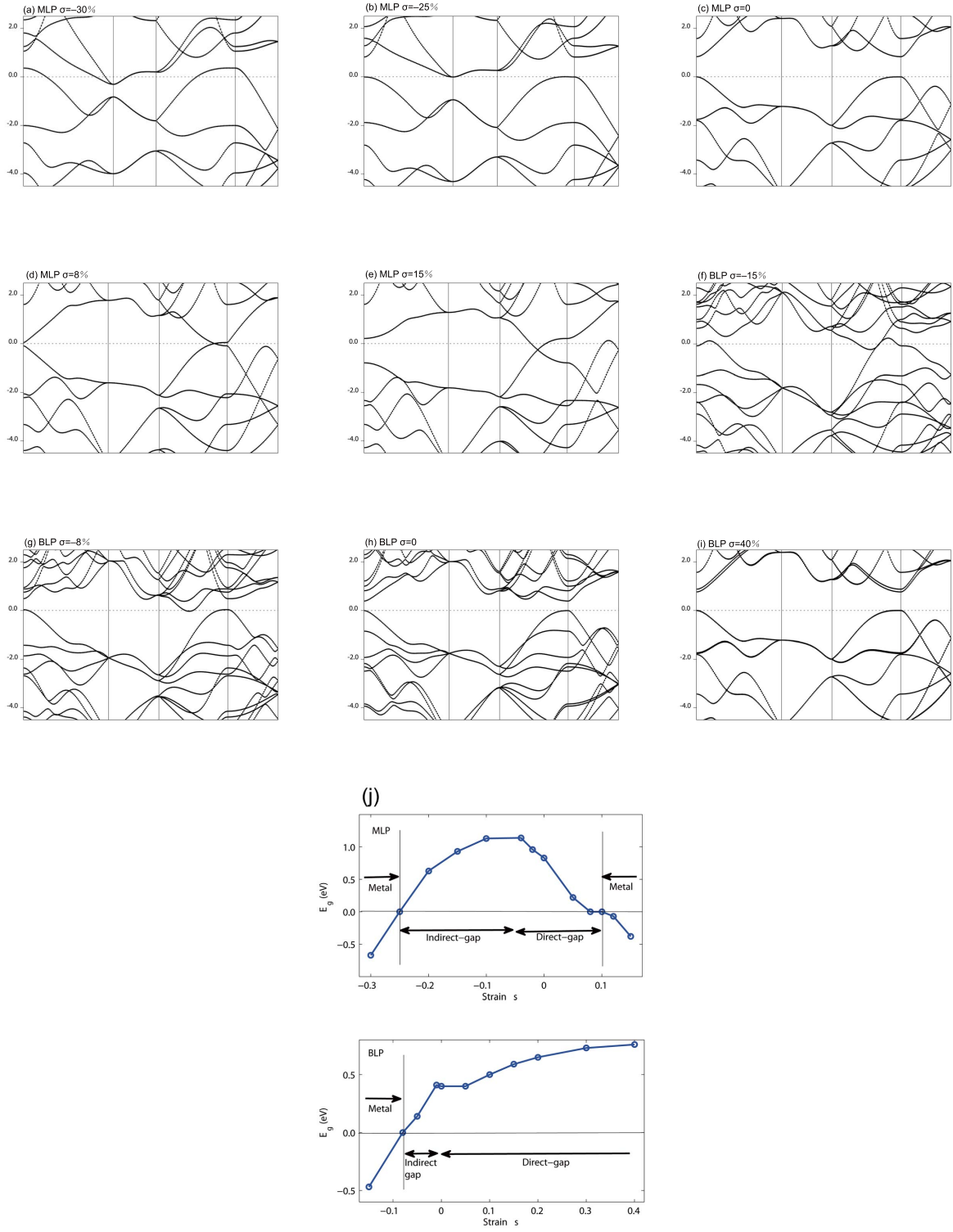


FIG. 2: The band structures of the strained phosphorene, (a)-(e) are for MLP; (f)-(i) are for BLP.

(j) The evolution of the band gap E_g with the strain.

three acoustic phonons branches. The Γ point modes can be decomposed as

$$\Gamma_{acoustic} = B_{1u} + B_{2u} + B_{3u} \quad (1)$$

and

$$\Gamma_{optical} = B_{1u} + B_{3u} + A_u + B_{1g} + B_{3g} + 2B_{2g} + 2A_g \quad (2)$$

Among optical modes, the A_u mode is silent, B_{1u} and B_{3u} are infrared active, while all others are Raman active. The structure of puckered layer remains the reflection symmetry in the y (zigzag) direction but breaks the reflection symmetry in the z and x directions. So the vibrations along the y direction are strict, while those along the z and x directions are mixed. B_{3g} and B_{1g} Raman modes correspond to the vibrations along y direction and their vibrational patterns are illustrated in Fig. 1c. For B_{3g} mode, the vibration of atom in the different layer is out-of-phase, but is in-phase in the same layer, i.e. two layers beating against each other. B_{1g} mode corresponds to the bond stretching modes from d_1 and d_2 covalent bonds. The other four Raman active modes have similar vibrational patterns along x and z directions, but each mode having mixed x and z characters. The Raman frequencies of free MLP are listed in Table 3. Our calculated frequencies are slightly smaller than those in Ref. [16]. For the free BLP, the frequencies of corresponding Raman active modes are also listed in Table 3. We find that the frequency shift between MLP and BLP is small except for A_g^1 and B_{2g}^2 modes, which vibrate mainly along the z direction. The frequencies of this two modes in BLP is smaller than those in MLP probably due to the attractive vdW interaction existed in BLP.

The phonon dispersion of free MLP calculated by the density functional perturbation theory is presented in Fig. 3 (a), which compares very well with previous calculations.^{10,16} Near the Γ point, two in-plane acoustic modes exhibit linear dispersions, while the off-plane acoustic mode exhibits a parabolic dispersion due to the 2D character of phosphorene. The vibrations of the bond-breathing modes occupy the high-frequency region, while the vibrations of layer-breathing modes and the acoustic modes occupy the low-frequency region. Fig. 3 (b) shows the calculated phonon dispersion of free BLP which has 24 phonon branches. The optical branches have small splitting and are nearly double degenerate due to the weak interlayer interaction. Near the Γ point, the splitting has an appreciable magnitude. Three branches from the opposite vibrations of two puckered layers (i.e. layer-breathing modes) deviate from three acoustic branches. From Fig. 3a and 3b, we can see that there is no

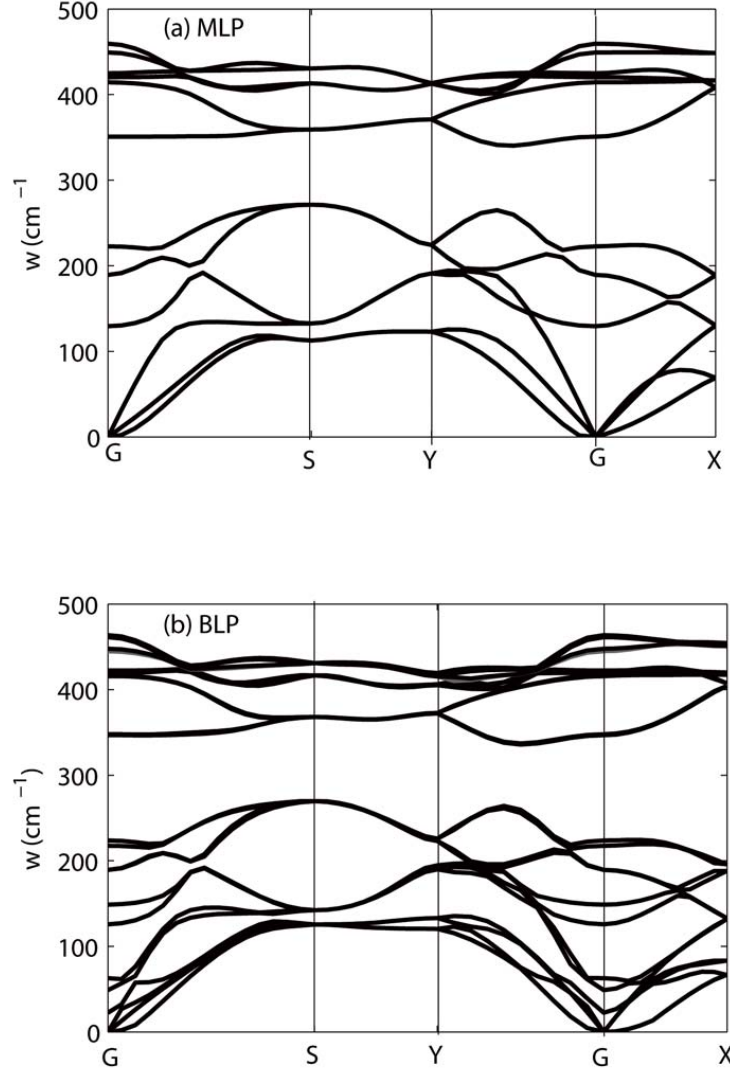


FIG. 3: The phonon dispersion of free MLP (a) and BLP (b).

imaginary frequency in the full phonon spectra, indicating the dynamical stability for both free-standing MLP and BLP. This conclusion is in good agreement with the experiment. Raman spectroscopy and transmission electron microscopy measurements show that the exfoliated flakes of BP are stable even in free-standing form.¹⁵

When vertical strain is increased to a certain value, we find phosphorene becomes unstable. For MLP, there appears imaginary frequency in the phonon dispersions when tensile

strain reaches 15% and compressive strain reaches 4%. The appearance of imaginary frequency of phonon modes indicates the dynamical instability under such strain. The dynamical stable range of MLP for strain σ is about $(-3\%, 12\%)$. Within this range, the frequencies of Raman active modes under several strains are also listed in Table 3. The response of each Raman mode to strain is not the same. Four modes ($B_{1g}, A_g^1, B_{2g}^1, B_{2g}^2$) exhibit monotonic change: their frequencies are red shifted under tensile strain and blue shifted under compressive strain. Among them, A_g^1, B_{2g}^2 modes which are vibrated mainly along the z direction have prominent shifts. The other two Raman modes exhibit nonmonotonic change. B_{3g} mode exhibits an abnormal red shift under small compressive strain. This is possibly due to the fact that the flattening of the puckered layer under compressive strain is in favor of the opposite vibrations of two layers along the zigzag chain. A_g^2 mode exhibits a nonmonotonic shift under tensile strain. Its frequency decreases at small tensile strain and then increases with increasing tensile strain. This abnormal behavior can be understood from the following: A_g^2 mode corresponds to the vibration of d_1 bond-breathing mainly along x direction. The lattice constant a is contracted when vertical tensile strain is applied. When the effect of this contraction of a dominates over the effect of increase of thickness of phosphorene, it will enhance the interatomic interactions, resulting in the increase of frequency of A_g^2 mode.

For BLP, we find its dynamical stable range for strain σ is wider than that of MLP. When compressive strain reaches 8%, imaginary frequency appears in the phonon dispersion along Γ -X direction. Within the stable dynamical range for strain σ , the frequencies of Raman active modes are also listed in Table 3. Under compressive strain, B_{3g} mode exhibits an abnormal red shift as in the case of MLP, while the frequencies of other Raman modes are blue shifted as expected as usual. BLP is still stable when tensile strain reaches 40%. As discussed above, large tensile strain only results in large interlayer distance with other geometric parameters in close to those in the MLP. Then BLP may be regarded as two nearly independent MLPs, which are stable in free-standing form as discussed above. Under the wide range of tensile strain, the changes of frequencies of four modes ($B_{3g}, B_{1g}, A_g^2, B_{2g}^1$) are all very small. This shows that the vertical tensile strain has little effect on the in-plane vibrational modes. With the increase of tensile strain, A_g^1, B_{2g}^2 modes vibrated mainly along the z direction are red shifted at first as expected, but they are then blue shifted. This abnormal blue shift may be due to the decrease of attractive vdW interaction at large interlayer distance.

D. Superconductivity by adjusting the interlayer distance

The above phonon calculations show that BLP is dynamical unstable when it achieves the transition from semiconductor to metal. Here we propose that stable metal phase or even a BCS superconductor can be achieved by adjusting the interlayer distance of BLP. We fix the interlayer distance at different given values, the unit cell and other atomic positions are then relaxed. Since the results with increasing the interlayer distance are very similar to those in the tensile strained BLP, next we only discuss the opposite case.

When the interlayer distance $0.6d_0 < d < d_0$ (d_0 is the interlayer distance of free BLP), our calculations show that the lattice constant a increases slightly, d_2 and θ_2 show only a weak variation, while the lattice constant b , d_1 and θ_1 hardly change. This means that the puckered character of BLP remains and changes little at this range of interlayer distance. When $d < 0.6d_0$, the structure of BLP starts to change substantially. The calculations of band structure show that the band gap E_g goes to zero when $d = 0.85d_0$. Keeping on decreasing the interlayer distance will result in the transition from semiconductor to metal. The calculations of phonon show that BLP is dynamical unstable when d is $0.65d_0$ or less. So the range of d for the stable metal phase of BLP is about $0.65d_0 < d < 0.85d_0$.

The Eliashberg spectral function $\alpha^2F(\omega)$ depends directly on the EP matrix element, $g_{\mathbf{k}+\mathbf{q},\mathbf{j}';\mathbf{k},\mathbf{j}}^{\mathbf{q}\nu}$, which can be determined self-consistently using linear response theory. By plotting $\alpha^2F(\omega)$ we can estimate the relative strength of the EP coupling. The phonon density of states $F(\omega)$ and $\alpha^2F(\omega)$ are plotted in Fig. 4 for three different interlayer distances, which are within the range of stable metal phase of BLP. When $d = 0.8d_0$, $d = 0.75d_0$ and $d = 0.7d_0$, $F(\omega)$ is very similar, while $\alpha^2F(\omega)$ is different. With smaller interlayer distance, the Eliashberg spectral function $\alpha^2F(\omega)$ has a significantly enhanced peak at the low-frequency side. The characteristic phonon modes which dominate the EP coupling are just from the opposite vibrations of two puckered double layers. So we speculate that the interlayer vdW attractive interaction may play an important role in enhancing the EP coupling of BLP with smaller interlayer distance.

The superconducting temperature T_c can be estimated from the Allen-Dynes modified McMillan equation²²:

$$T_C = \frac{\omega_{ln}}{1.2} \exp \left(-\frac{1.04(1 + \lambda)}{\lambda - \mu^*(1 + 0.62\lambda)} \right), \quad (3)$$

where ω_{ln} is the logarithmically averaged frequency, μ^* is the Coulomb repulsion parameter.

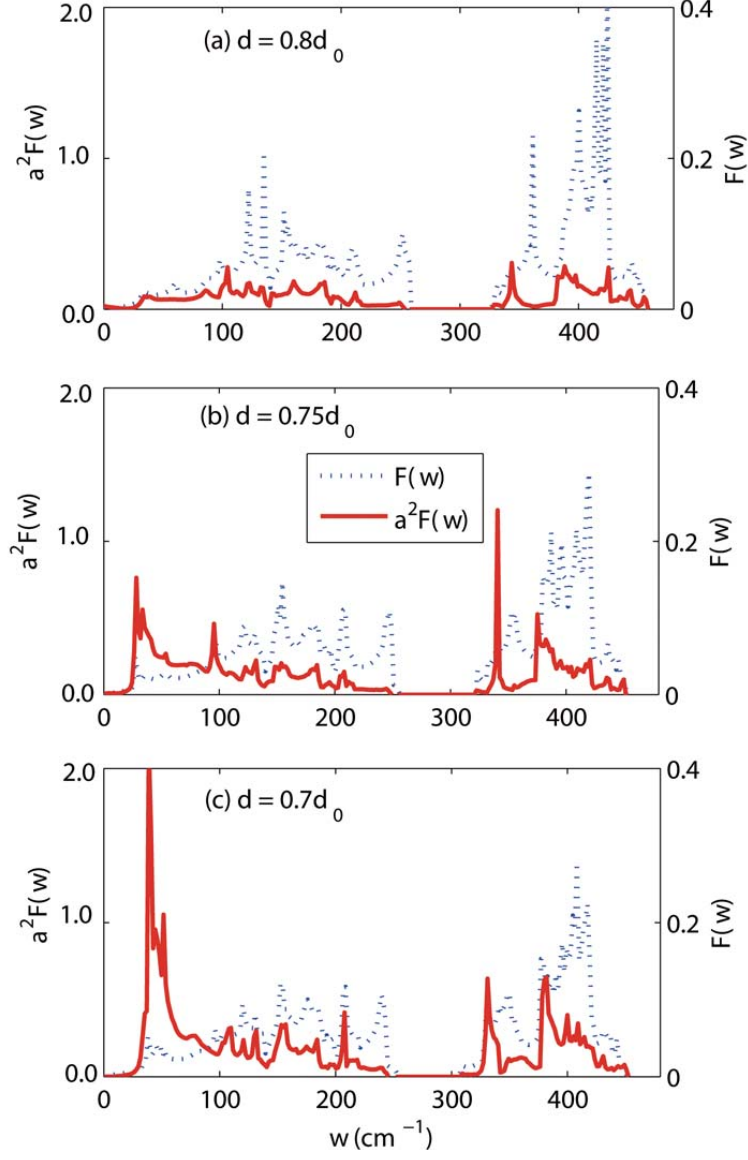


FIG. 4: The phonon density of states $F(\omega)$ and the Eliashberg spectral function $\alpha^2 F(\omega)$ for BLP at three different interlayer distances.

The calculated electronic densities of states at Fermi level $N(E_F)$, EP coupling constant λ , ω_{ln} and the estimated T_C when taking $\mu^* = 0.1$ are summarized in Table 4. With the decrease of interlayer distance, BLP apparently becomes more metallic and results in the

increase of $N(E_F)$. Most remarkably, we see λ increases dramatically. The increase of both $N(E_F)$ and λ is favorable to enhance T_C . When $d = 0.7d_0$, λ reaches as high as 1.45 and the estimated T_C is about 10K. The superconductivity of BP was reported early under high pressure.^{5,6} Our results suggest that BLP may become a good BCS superconductor by adjusting the interlayer distance.

IV. SUMMARY

In conclusion, MLP and BLP under vertical strain are studied by density functional and density-functional perturbation theory. The results show that the electronic structure of thin BP is very sensitive to its thickness and the strain applied. The change is extensive. It can increase direct band gap, decrease indirect band gap or realize the transition from semiconductor to metal, which help to tailor materials in a variety of settings, from infrared optoelectronics to high-mobility quantum transport. The shift of zone-center Raman active modes for strained phosphorenes is analyzed and explained combining the relaxation of geometric structure. Our study clearly show that both MLP and BLP in free-standing form are dynamical stable. However, material becomes dynamical unstable with large vertical strain. We find that the dynamical stable range for strain σ in BLP is wider than that in MLP due to add the interlayer weak vdW coupling, this additional freedom. This information is essential for future device fabrication and potential applications of phosphorene. Furthermore we also find that BLP may become a good BCS superconductor by adjusting the interlayer distance.

V. ACKNOWLEDGMENTS

The authors acknowledge the support of the Natural Science Foundation of Jiangsu Province in China under Grant No. BK20141441, the State Key Program for Basic Researches of China (2014CB921103 and 2010CB923404), the National "Climbing" Program of China (91021003), and the National Science Foundation of Jiangsu Province (BK2010012).

¹ C. M. Park and H. J. Sohn, Adv. Mater. 19, 2465 (2007).

- ² L. Q. Sun, M. J. Li, K. Sun, S. H. Yu, R. S. Wang, and H. M. Xie, *J. Phys. Chem. C*, 116,14772 (2012).
- ³ Y. Ktayama, T. Mizutani, W. Utsumi, O. Shimomura, M. Yamakata, K. Funakoshi, *Nature*, 403,170 (2000).
- ⁴ C. A. Vanderborgh and D. Schifer, *Phys. Rev. B*, 49, 9595 (1989).
- ⁵ H. Kawamura, I. Shirotani, K. Tachikawa, *Solid State Commun*, 49, 879, (1984).
- ⁶ J. Wittig, B. T. Matthias, *Science* 160, 994, (1968).
- ⁷ L. Li, Y. Yu, G. J. Ye, Q. Ge, X. Ou, H. Wu, D. Feng, X. H. Chen and Y. Zhang, *Nature Nanotech.* 9, 372 (2014).
- ⁸ H. Liu, A. T. Neal, Z. Zhu, D. Tománek and P. D. Ye, *ACS Nano* 8, 4033 (2014).
- ⁹ S. P. Koenig, R. A. Doganov, H. Schmidt, A. H. Castro Neto and O. Barbaros, *Applied Physics Letters* 104, 103106 (2014).
- ¹⁰ Ruixiang Fei, Alireza Faghaninia, Ryan Soklaski, Jia-An Yan, Cynthia Lo, Li Yang, Preprint at <http://arxiv.org/abs/1405.2836> (2014).
- ¹¹ M. S. Scheurer, J. Schmalian, Preprint at <http://arxiv.org/abs/1404.4030> (2014).
- ¹² R. W. Keyes, *Phys. Rev.* 92, 580 (1953).
- ¹³ J. S. Qiao, X. H. Kong, Z. X. Hu, F. Yang, W. Ji, *Nature Communications* 5, 4475 (2014)
- ¹⁴ A. S. Rodin, A. Carvalho, and A. H. Castro Neto, *Phys. Rev. Lett.* 112, 176801 (2014).
- ¹⁵ A. Castellanos-Gomez *et al.*, *2D Matererials* 1, 025001 (2014).
- ¹⁶ R. X. Fei and L. Yang, *Applied Physics Letters* 105, 083120 (2014).
- ¹⁷ P. Giannozzi *et al.*, *J. Phys. Condens. Matter* **21** (2009) 395502. and <http://www.quantum-espresso.org>
- ¹⁸ S. Grimme, *J. Comput. Chem.* 27, 1787,(2006).
- ¹⁹ Y. Takao, *Physica (Amsterdam)* 105B, 93 (1981).
- ²⁰ Y. L. Du, C. Y. Ouyang, S. Q. Shi, and M. S. Lei, *J. Appl. Phys.* 107, 093718 (2010).
- ²¹ G. Z. Qin, Z. Z. Qin, S. Y. Yue, H. J. Cui, Q. R. Zheng, Q. B. Yan, and G. Su, Preprint at <http://arxiv.org/abs/1406.0261> (2014).
- ²² P. B. Allen and R. C. Dynes, *Phys. Rev. B* **12**, 905 (1975).

Figure Caption

Figure 1. The top (a) and side views (b) of the atomic structure of phosphorene. (c) Vibrational pattern of B_{3g} and B_{1g} modes.

Figure 2. The band structures of the strained phosphorene, (a)-(e) are for MLP; (f)-(i) are for BLP. (j) The evolution of the band gap E_g with the strain.

Figure 3. The phonon dispersion of free MLP (a) and BLP (b).

Figure 4. The phonon density of states $F(\omega)$ and the Eliashberg spectral function $\alpha^2 F(\omega)$ for BLP at three different interlayer distances.

TABLE I: Structural parameters of bulk BP.

	a(Å)	b(Å)	c(Å)	d ₁ (Å)	d ₂ (Å)	θ ₁	θ ₂
Exp. (Ref.19)	4.376	3.314	10.478	2.224	2.244	96.34°	102.09°
Theo.(Ref.20)	4.422	3.348	10.587	2.238	2.261	96.85°	102.31°
This work (with vdW)	4.398	3.325	10.429	2.227	2.257	96.56°	102.20°
This work (without vdW)	4.503	3.311	11.033	2.227	2.261	96.07°	103.03°

TABLE II: Structural parameters of strained MLP and BLP.

σ	a(Å)	b(Å)	d ₁ (Å)	d ₂ (Å)	θ ₁	θ ₂
MLP						
0.15	4.281	3.293	2.198	2.545	97.04°	100.27°
0.10	4.379	3.294	2.210	2.451	96.38°	101.24°
0.05	4.441	3.311	2.224	2.355	96.22°	102.04°
0.00	4.525	3.311	2.222	2.255	96.35°	103.35°
-0.05	4.671	3.302	2.215	2.200	96.40°	105.10°
-0.10	4.904	3.292	2.201	2.159	96.81°	107.74°
-0.25	5.729	3.287	2.176	2.151	98.14°	116.00°
BLP						
0.40	4.527	3.308	2.221	2.256	96.27°	103.33°
0.15	4.523	3.308	2.222	2.261	96.21°	103.31°
0.10	4.513	3.310	2.223	2.265	96.20°	103.16°
0.05	4.486	3.311	2.225	2.267	96.19°	102.92°
0.00	4.485	3.314	2.225	2.259	96.24°	102.98°
-0.05	4.505	3.320	2.226	2.233	96.46°	103.33°
-0.10	4.607	3.324	2.225	2.208	96.67°	104.41°
-0.20	4.994	3.390	2.220	2.199	99.55°	107.91°

TABLE III: Frequencies (cm^{-1}) of Raman modes of strained phosphorene.

σ	B_{3g}	B_{1g}	B_{2g}^1	B_{2g}^2	A_g^1	A_g^2
MLP ^a						
0.00	196	433	226	427	368	456
MLP ^b						
0.12	170.1	417.4	152.5	276.6	147.8	455.6
0.10	175.2	415.8	162.8	297.1	152.0	444.0
0.08	180.9	416.2	175.9	320.1	170.1	433.5
0.05	187.2	418.1	196.0	357.8	266.9	431.4
0.00	188.2	421.9	222.9	424.5	349.7	449.9
-0.02	187.8	424.3	226.8	437.5	354.5	459.2
-0.03	185.4	425.5	230.1	449.0	359.2	466.6
BLP ^b						
0.40	188.9	422.3	221.9	423.4	349.5	449.5
0.15	189.0	421.7	221.4	420.3	345.4	448.2
0.10	189.1	421.2	221.1	418.0	344.9	448.5
0.05	188.9	421.2	220.0	414.7	341.5	446.2
0.00	188.1	422.6	221.2	419.9	346.7	450.3
-0.03	186.2	424.2	226.3	431.0	353.6	452.6
-0.05	185.8	426.0	228.1	436.7	357.8	463.0

^aRef. 16.

^bThis work

TABLE IV: The calculated electronic densities of states at Fermi level $N(E_F)$, EP coupling constant λ , the logarithmically averaged frequency ω_{ln} and the estimated T_C for BLP at three different interlayer distances.

d/d_0	$N(E_F)(States/eV)$	λ	$\omega_{ln}(K)$	$T_C(K)$
0.80	0.68	0.32	183.2	0.2
0.75	0.86	0.85	107.9	5.7
0.70	1.08	1.45	96.1	10.6